JACS
JOURNAL OF THE AMERICAN CHEMICAL SOCIETY
Communication
pubs.acs.org/JACS

Reductively Cleavable Nanocaplets for siRNA Delivery by Template-Assisted Oxidative Polymerization

P. K. Hashim,[†] Kou Okuro,*[,†] Shigekazu Sasaki,[‡] Yasutaka Hoashi,[‡] and Takuzo Aida*[,†,§]

[†]Department of Chemistry and Biotechnology, School of Engineering, The University of Tokyo, 7-3-1 Hongo, Bunkyo-ku, Tokyo 113-8656, Japan

[‡]Pharmaceutical Research Division, Takeda Pharmaceutical Company Limited, 26-1, Muraoka-Higashi 2-chome, Fujisawa, Kanagawa 251-8555, Japan

[§]Riken Center for Emergent Matter Science, 2-1 Hirosawa, Wako, Saitama 351-0198, Japan

Supporting Information

ABSTRACT: A series of water-soluble telechelic dithiol monomers bearing multiple guanidinium ion (Gu^+) units in their main chains were synthesized for packaging siRNA by template-assisted oxidative polymerization at their thiol termini. In the presence of siRNA, oxidative polymerization of $^{TEG}Gu_4$ affords a uniform-sized (7 ± 2 nm) nanocaplet containing siRNA ($P^{TEG}Gu_4 \supset$siRNA; $P^{TEG}Gu_4$ = polymerized $^{TEG}Gu_4$). When this small conjugate is incubated with live cells, cellular uptake occurs, and the nanocaplet undergoes depolymerization in the reductive cytosolic environment to liberate the packaged siRNA. Consequently, gene expression in the live cells is suppressed.

The molecular design of effective carriers for small interfering RNA (siRNA) that can mimic a "natural virus" containing a single genome in a thin capsid shell is attractive for the application of RNA interference (RNAi)-based gene therapy.[1,2] For the delivery, siRNA is hybridized with carriers based on lipids or polymers, where polydisperse aggregates of 100−200 nm in diameter usually form.[3] Although this size regime is appropriate for long-term retention in a bloodstream, most siRNA conjugates are trapped by liver. For enabling the penetration of siRNA into other tissues, small siRNA/carrier conjugates are often considered.[4] Such small conjugates can plausibly ensure deeper penetration of tissues through endothelial fenestrations (60−80 nm)[5] or intercellular gaps (∼10 nm).[6] Previous efforts have produced a few examples of siRNA/carrier conjugates of 20−30 nm in size, each of which utilizes designed lipid components,[7] star-shaped polymers,[8] or polymer shells.[9] However, the construction of a siRNA/carrier conjugate smaller than 10 nm comprising the characteristics (size, charge, and degradability) of "small molecule drugs" remains a big challenge. Here, we successfully produced a small siRNA/carrier conjugate with a uniform size of 7 ± 2 nm by oxidative polymerization of a water-soluble telechelic dithiol monomer carrying multiple guanidinium ion (Gu^+) pendants (Figure 1) in the presence of siRNA as a template (Figure 2). This conjugate is reductively cleavable to liberate packaged siRNA.

We previously developed water-soluble dendritic[10a−e] and linear[10f,g] molecular glues bearing multiple Gu^+ units in their side chains and main chains, respectively. These molecular glues adhere strongly to proteins,[10a,c,e,g] phospholipid membranes,[10d] and clay nanosheets[10b,f] via the formation of multiple salt bridges between their Gu^+ units and oxyanionic groups located on the targets. In the present study, we synthesized a series of glue monomers (Figure 1) that are likely adhesive to siRNA because their Gu^+ units, separated by a 7.4-Å long ether spacer (Figure S1), possibly form salt bridges efficiently with the phosphate groups of siRNA, which are located at regular intervals of 6−7 Å along the siRNA strand.[11] The disulfide polymers obtained by oxidative polymerization can be reductively cleaved (Figure 2) in glutathione (GSH)-rich media such as cytoplasm.

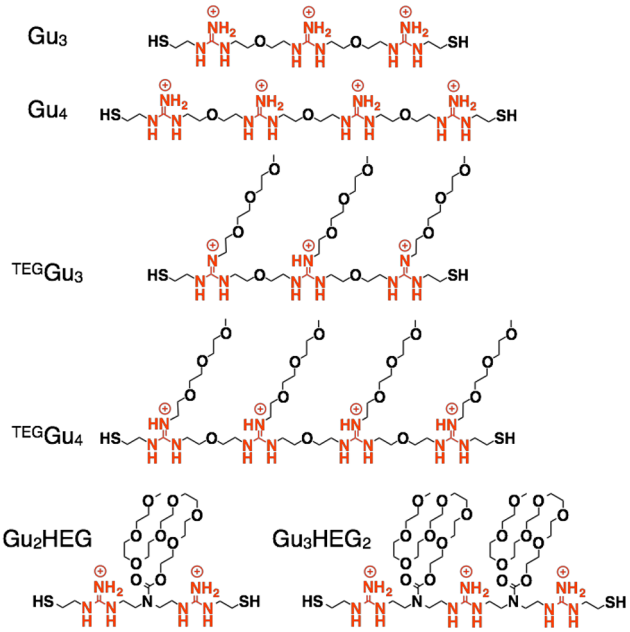

Figure 1. Molecular structures of guanidinium ion (Gu^+)-appended telechelic monomers carrying thiol (SH) termini without side chains (Gu_3 and Gu_4), those with triethylene glycol (TEG) side chains on the Gu^+ units ($^{TEG}Gu_3$ and $^{TEG}Gu_4$), and with heptaethylene glycol (HEG) side chains between the Gu^+ units (Gu_2HEG and Gu_3HEG_2).

Received: August 24, 2015
Published: December 9, 2015

DOI: 10.1021/jacs.5b08948
J. Am. Chem. Soc. 2015, 137, 15608−15611

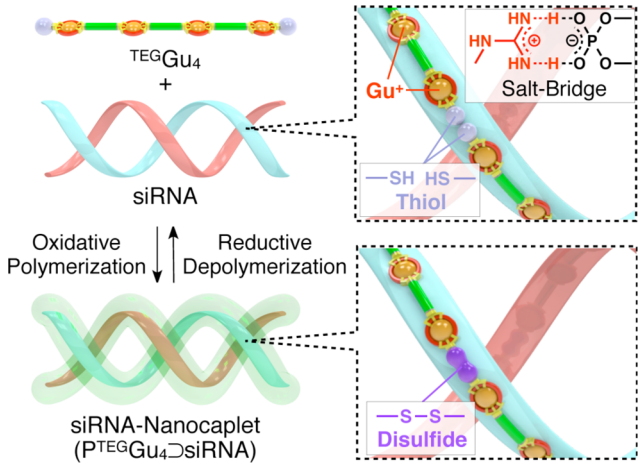

Figure 2. Oxidative polymerization of $^{TEG}Gu_4$ with siRNA as the template. $^{TEG}Gu_4$ adheres to siRNA via the formation of multiple Gu^+/phosphate ion (PO_4^-) salt bridges and undergoes oxidative polymerization to form a siRNA-containing $P^{TEG}Gu_4$ nanocaplet ($P^{TEG}Gu_4\supset$siRNA). $P^{TEG}Gu_4$ depolymerizes under reductive conditions.

The monomers in Figure 1 were synthesized according to the procedures described in the Supporting Information and characterized unambiguously using a variety of analytical methods. In agarose gel electrophoresis, siRNA (10 μL, 2.2 μM), under conditions employed (see Supporting Information, Chapter 5), migrated according to its net negative charges (Figure 3a, N/P = 0). However, no siRNA migration was

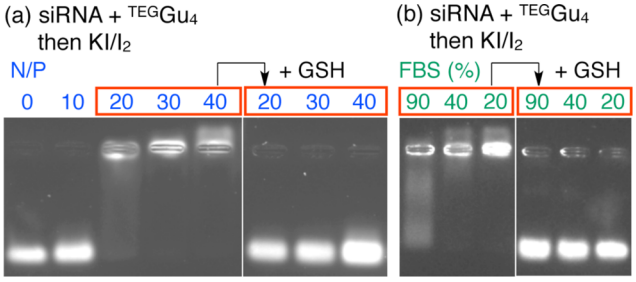

Figure 3. Agarose gel electrophoresis profiles of mixtures of siRNA (2.2 μM) and $^{TEG}Gu_4$ (0–0.9 mM) upon treatment with KI/I_2 (0–1.2 mM) in HEPES buffer (100 mM, pH 8.5) followed by glutathione (GSH; 5 mM, pH 7.0) (a) without and (b) with fetal bovine serum (FBS; 20, 40, and 90%). siRNA and $^{TEG}Gu_4$ were mixed at (a) N/P = 0–40 and (b) 40.

observed after the incubation with $^{TEG}Gu_4$ (N/P > 20) in HEPES buffer (100 mM, pH 8.5; 30 min at room temperature) containing KI/I_2 as an oxidant (Figure 3a). By contrast, when KI/I_2 was omitted in the above procedure, siRNA migration was not suppressed even though $^{TEG}Gu_4$ was present in large excess (N/P = 80; Figure S2). This result indicates that $P^{TEG}Gu_4$ formed by the oxidative polymerization of $^{TEG}Gu_4$ with KI/I_2 forms a conjugate with siRNA ($P^{TEG}Gu_4\supset$siRNA) and effectively neutralizes its negative charges. Accordingly, when $P^{TEG}Gu_4\supset$siRNA (N/P = 20–40) was incubated with GSH (5 mM) for 1 min in loading buffer (5 mM HEPES, 1 mM EDTA, 10% glycerol, pH 7.0) at room temperature, the gel electrophoresis profile was identical to that of intact siRNA before the polymerization (Figure 3a). Thus, the $P^{TEG}Gu_4$ part of $P^{TEG}Gu_4\supset$siRNA was cleaved reductively to liberate siRNA.

We examined other monomers listed in Figure 1. Similarly to $^{TEG}Gu_4$, shorter-chain $^{TEG}Gu_3$ retarded the electrophoretic migration of siRNA in an agarose gel (N/P = 20) after the oxidative polymerization with KI/I_2 (Figure S3). By contrast, when Gu_3 (Figure S5) and Gu_4 (Figure S6) that are devoid of triethylene glycol (TEG) chains were likewise mixed with siRNA, a precipitate formed rapidly even at N/P = 20. Gu_2HEG and Gu_3HEG_2 are highly water-soluble because of a long heptaethylene glycol (HEG) side chain between the Gu^+ units in their main chains. However, these monomers also yielded precipitates when mixed with siRNA (Figures S7 and S8) in the presence of KI/I_2.

$P^{TEG}Gu_4\supset$siRNA was uniform in size. Figure 4, panel a shows a cryogenic transmission electron microscopy (cryo-

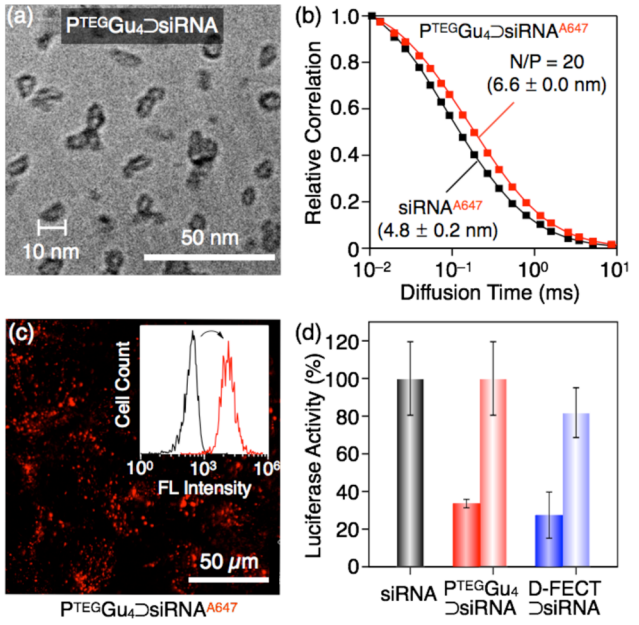

Figure 4. (a) A cryogenic TEM image of $P^{TEG}Gu_4\supset$siRNA (N/P = 20) in HEPES buffer (20 mM, pH 8.5). (b) Relative autocorrelation (squares) and fitting (solid curves) profiles in FCS of $P^{TEG}Gu_4\supset siRNA^{A647}$ at N/P = 0 (black) and 20 (red) in HEPES buffer (20 mM, pH 7.4) at 25 °C. Hydrodynamic diameters (d_h) were calculated from the diffusion coefficients, which were determined by autocorrelation fitting to a triplet state model. (c) A confocal laser scanning microscopy image (λ_{ext} = 638 nm) of Hep3B cells after a 24-h incubation at 37 °C in minimal essential medium (MEM; 10% FBS) containing $P^{TEG}Gu_4\supset siRNA^{A647}$ ([$siRNA^{A647}$] = 0.2 μM, N/P = 30). Inset: Flow cytometry histograms (λ_{ext} = 640 nm) of Hep3B cells before (black) and after (red) incubation with $P^{TEG}Gu_4\supset siRNA^{A647}$ for 24 h. (d) Normalized luciferase activities of Hep3B-luc cells using the PicaGene LT 2.0 luciferase assay. Here, Hep3B-luc cells were incubated at 37 °C in MEM (10% FBS) containing $siRNA^{A647}$ (0.2 μM, gray bar), $P^{TEG}Gu_4\supset siRNA^{A647}$ (0.2 μM, N/P = 30; $siRNA^{A647}$ and mis-siRNA, red and light red bars, respectively), or a mixture of $siRNA^{A647}$ and DharmaFECT (0.2 μM; $siRNA^{A647}$ and mis-siRNA, blue and light blue bars, respectively) for 24 h, followed by incubation for 48 h at 37 °C in MEM (10% FBS).

TEM) image of a polymerization mixture of $^{TEG}Gu_4$ in the presence of siRNA (N/P = 20). Objects that can be referred to as siRNA-containing "nanocaplets" with diameters of <10 nm were observed (Figure 4a). We utilized siRNA fluorescently labeled with Alexa Fluor 647 ($siRNA^{A647}$) as a template for the oxidative polymerization of $^{TEG}Gu_4$ and found that the hydrodynamic diameter (d_h) of the nanocaplet formed at N/

DOI: 10.1021/jacs.5b08948
J. Am. Chem. Soc. 2015, 137, 15608–15611

P = 20, as determined by fluorescence correlation spectroscopy (FCS), was 6.6 ± 0.0 nm (Figure 4b). This value is reasonable considering that siRNA^{A647} possesses a slightly smaller d_h value of 4.8 ± 0.2 nm. Even at a higher N/P ratio such as 40, the caplets remained small (d_h = 7.6 ± 0.3 nm, Figure S10d). The number of siRNA molecules in one caplet (N/P = 20−40) was nearly unity, as evaluated by FCS[12] (Table S1). The molar equivalent of polymerized $^{TEG}Gu_4$ per siRNA, quantified after reductive cleavage of the disulfide bonds in $P^{TEG}Gu_4$⊃siRNA (N/P = 30), was 8.8 (Table S3), which is close to the expected value of 10. These results support the mechanism of template-assisted polymerization with siRNA. When siRNA was added after the polymerization of $^{TEG}Gu_4$ with KI/I_2, TEM (Figure S9d) revealed the formation of polydisperse aggregates with a larger average size (∼35 nm). These results were also supported by dynamic light scattering (DLS) and zeta potential analysis (Figure S13).

Advantageously for delivery purposes, the $P^{TEG}Gu_4$⊃siRNA conjugate (e.g., N/P = 40) obtained by template-assisted oxidative polymerization (Figure 2) did not disassemble in the presence of fetal bovine serum (FBS) ([FBS] = 20, 40, and 90%; Figure 3b). However, when the $P^{TEG}Gu_4$⊃siRNA conjugate was heated at 40 °C for 48 h in HEPES buffer (20 mM, pH = 7) containing $ZnCl_2$ (50 mM) for selective hydrolysis of siRNA,[13] the $P^{TEG}Gu_4$ nanocaplet was isolated from $P^{TEG}Gu_4$⊃siRNA. Liquid chromatography−mass spectrometry (LC−MS) analysis of the reaction mixture on an OD column, by reference to monomer $^{TEG}Gu_4$ (Figure S16, m/z = 383.90, z = 3), revealed a set of ion peaks assignable up to hexameric $^{TEG}Gu_4$ (Figure S14, m/z = 627.92, z = 11). Because the total number of negative ions on each siRNA strand is 21, the formation of oligomers up to the hexamer (number of Gu^+ = 24) is reasonable for the mechanism of template-assisted polymerization. When the polymerization of $^{TEG}Gu_4$ was attempted without siRNA under conditions otherwise identical to the above, ion peaks assignable only up to dimeric $^{TEG}Gu_4$ (Figure S15, m/z = 460.68, z = 5) were observed. Despite the strong ionic interaction in $P^{TEG}Gu_4$⊃siRNA, its circular dichroism (CD) spectrum in HEPES buffer (10 mM) at 25 °C was analogous to the spectrum of intact siRNA (Figure S17), indicating that siRNA packaged in the nanocaplet maintained its intrinsic secondary structure.

$P^{TEG}Gu_4$⊃siRNA was efficiently taken up into living cells. Human hepatocellular carcinoma Hep3B cells (1.0×10^4 cells/well) were incubated for 24 h at 37 °C in minimal essential medium (MEM, 10% FBS; 200 μL) containing $P^{TEG}Gu_4$⊃siRNA^{A647} ([siRNA^{A647}] = 0.2 μM, N/P = 30) and then subjected to confocal laser scanning microscopy (CLSM; λ_{ext} = 638 nm). As shown in Figure 4, panel c, the cells became fluorescent, indicating the incorporation of siRNA^{A647} within the Hep3B cells. By contrast, the cells barely fluoresced when incubated with siRNA^{A647} alone (0.2 μM) under conditions otherwise identical to the above (Figure S18). Accordingly, in flow cytometry (λ_{ext} = 640 nm), Hep3B cells treated with $P^{TEG}Gu_4$⊃siRNA^{A647} were 130-fold more emissive, on average, than the untreated cells (Figure 4c, inset). The high affinity of Gu^+ in the $P^{TEG}Gu_4$ nanocaplet toward oxyanionic groups abundant on the cell membrane plays a role in the cellular uptake of $P^{TEG}Gu_4$⊃siRNA.[14]

We next investigated the possibility of gene silencing. Mutant Hep3B cells stably expressing luciferase (Hep3B-luc) were incubated at 37 °C in MEM (10% FBS) containing $P^{TEG}Gu_4$⊃siRNA^{A647} ([siRNA^{A647}] = 0.2 μM, N/P = 30) for 24 h, followed by MEM (10% FBS) for 48 h. Then, the mixture was subjected to the luciferase activity assay using PicaGene LT 2.0 as a luminescence reagent (TOYO INK). As shown in Figure 4, panel d, Hep3B cells incubated with $P^{TEG}Gu_4$⊃siRNA exhibited a much smaller luciferase activity (Figure 4d, red, 29%) than the reference cells incubated with siRNA (Figure 4d, black). The luciferase gene suppression level of $P^{TEG}Gu_4$⊃siRNA was comparable to that of a commercial transfection reagent DharmaFECT (Figure 4d, blue, 27%). This result is noteworthy because the amount of uptaken siRNA with the $P^{TEG}Gu_4$ caplet was five-fold smaller than that with DharmaFECT (Table S4). Later, we found that a rather poor cellular uptake activity of $P^{TEG}Gu_4$⊃siRNA^{A647} can be improved when the nanocaplet is connected to arginine peptide-Arg6 (Table S4, Figures S18 and S23).

To confirm whether the observed suppression in Figure 4d (red) is indeed caused by RNAi, we used mismatch siRNA (mis-siRNA) that does not induce RNAi for the luciferase gene. When $P^{TEG}Gu_4$⊃mis-siRNA ([mis-siRNA] = 0.2 μM) was used, the luciferase activity was not suppressed at all (Figure 4d, light red bar) under conditions otherwise identical to the above, indicating that the observed suppression in Figure 4, panel d (red) is mostly due to RNAi. In fact, by using the Cell Counting Kit-8 assay, we confirmed that $P^{TEG}Gu_4$⊃siRNA^{A647} is not cytotoxic even in a higher concentration range of siRNA^{A647} ([siRNA^{A647}] ≤ 0.5 μM; Figure S22). In contrast, when DharmaFECT⊃mis-siRNA was used, the luciferase activity was considerably suppressed (∼20%; Figure 4d, light blue bar).

In conclusion, we developed siRNA-containing nanocaplets ($P^{TEG}Gu_4$⊃siRNA, 7 ± 2 nm) by template-assisted polymerization of $^{TEG}Gu_4$ that are adhesive to siRNA (Figure 2). $P^{TEG}Gu_4$⊃siRNA is taken up into live cells, where the nanocaplet is reductively cleaved by the action of glutathione, thus liberating siRNA in the cytoplasm. Consequently, RNAi occurs and suppresses gene expression. This nanocaplet is expected to potentially pass through the gap between endothelial cells for in vivo gene knockdown. For in vivo testing, we need to consider a possible effect of the glomerular basement membrane (GBM) in kidney, although its filtration cutoff (≤ 4 nm)[15] is smaller than $P^{TEG}Gu_4$⊃siRNA (7 ± 2 nm). Because the blood−brain barrier (BBB) admits only very small particles,[16] a study on the delivery of siRNA to brain tissue using our nanocaplet is also one of the subjects worthy of further investigation.

■ ASSOCIATED CONTENT

Supporting Information

The Supporting Information is available free of charge on the ACS Publications website at DOI: 10.1021/jacs.5b08948.

Synthesis of Gu^+ monomers, their spectral data, and related experimental procedures; TEM images; electrophoresis profiles; FCS profiles; DLS profiles; LC−MS charts; CLSM images (PDF)

■ AUTHOR INFORMATION

Corresponding Authors

*okuro@macro.t.u-tokyo.ac.jp

*aida@macro.t.u-tokyo.ac.jp

Notes

The authors declare no competing financial interest.

DOI: 10.1021/jacs.5b08948
J. Am. Chem. Soc. 2015, 137, 15608−15611

■ ACKNOWLEDGMENTS

We appreciate Y. Sakaguchi and Prof. T. Suzuki (The University of Tokyo) for LC−MS analysis. This work was partially supported by a JSPS KAKENHI Grant-in-Aid for Young Scientists (B) (26810046) to K.O.

■ REFERENCES

(1) (a) Elbashir, S. M.; Harborth, J.; Lendeckel, W.; Yalcin, A.; Weber, K.; Tuschl, T. *Nature* **2001**, *411*, 494. (b) Fire, A.; Xu, S. Q.; Montgomery, M. K.; Kostas, S. A.; Driver, S. E.; Mello, C. C. *Nature* **1998**, *391*, 806.

(2) (a) Nguyen, J.; Szoka, F. C. *Acc. Chem. Res.* **2012**, *45*, 1153. (b) Kanasty, R.; Dorkin, J. R.; Vegas, A.; Anderson, D. *Nat. Mater.* **2013**, *12*, 967. (c) Miyata, K.; Nishiyama, N.; Kataoka, K. *Chem. Soc. Rev.* **2012**, *41*, 2562.

(3) (a) Wagner, E. *Acc. Chem. Res.* **2012**, *45*, 1005. (b) Wang, J.; Lu, Z.; Wientjes, M. G.; Au, J. L-S. *AAPS J.* **2010**, *12*, 492. (c) Buyens, K.; De Smedt, S. C.; Braeckmans, K.; Demeester, J.; Peeters, L.; van Grunsven, L. A.; de Mollerat du Jeu, X.; Sawant, R.; Torchilin, V.; Farkasova, K.; Ogris, M.; Sanders, N. N. *J. Controlled Release* **2012**, *158*, 362. (d) Tang, L.; Yang, X.; Yin, Q.; Cai, K.; Wang, H.; Chaudhury, I.; Yao, C.; Zhou, Q.; Kwon, M.; Hartman, J. A.; Dobrucki, I. T.; Dobrucki, L. W.; Borst, L. B.; Lezmi, S.; Helferich, W. G.; Ferguson, A. L.; Fan, T. M.; Cheng, J. *Proc. Natl. Acad. Sci. U. S. A.* **2014**, *111*, 15344. (e) Sykes, E. A.; Chen, J.; Zheng, G.; Chan, W. C. W. *ACS Nano* **2014**, *8*, 5696.

(4) Rozema, D. B.; Lewis, D. L.; Wakefield, D. H.; Wong, S. C.; Klein, J. J.; Roesch, P. L.; Bertin, S. L.; Reppen, T. W.; Chu, Q.; Blokhin, A. V.; Hagstrom, J. E.; Wolff, J. A. *Proc. Natl. Acad. Sci. U. S. A.* **2007**, *104*, 12982.

(5) (a) Takakura, Y.; Mahato, R. I.; Hashida, M. *Adv. Drug Delivery Rev.* **1998**, *34*, 93. (b) Cabral, H.; Matsumoto, Y.; Mizuno, K.; Chen, Q.; Murakami, M.; Kimura, M.; Terada, Y.; Kano, M. R.; Miyazono, K.; Uesaka, M.; Nishiyama, N.; Kataoka, K. *Nat. Nanotechnol.* **2011**, *6*, 815.

(6) Brink, P. R.; Valiunas, V.; Gordon, C.; Rosen, M. R.; Cohen, I. S. *Biochim. Biophys. Acta, Biomembr.* **2012**, *1818*, 2076.

(7) Rudorf, S.; Rädler, J. O. *J. Am. Chem. Soc.* **2012**, *134*, 11652.

(8) (a) Sizovs, A.; Song, X.; Waxham, M. N.; Jia, Y.; Feng, F.; Chen, J.; Wicker, A. C.; Xu, J.; Yu, Y.; Wang, J. *J. Am. Chem. Soc.* **2014**, *136*, 234. (b) Cho, H. Y.; Averick, S. E.; Paredes, E.; Wegner, K.; Averick, A.; Jurga, S.; Das, S. R.; Matyjaszewski, K. *Biomacromolecules* **2013**, *14*, 1262.

(9) Yan, M.; Liang, M.; Wen, J.; Liu, Y.; Lu, Y.; Chen, I. S. Y. *J. Am. Chem. Soc.* **2012**, *134*, 13542.

(10) (a) Okuro, K.; Kinbara, K.; Tsumoto, K.; Ishii, N.; Aida, T. *J. Am. Chem. Soc.* **2009**, *131*, 1626. (b) Wang, Q.; Mynar, J. L.; Yoshida, M.; Lee, E.; Lee, M.; Okuro, K.; Kinbara, K.; Aida, T. *Nature* **2010**, *463*, 339. (c) Okuro, K.; Kinbara, K.; Takeda, K.; Inoue, Y.; Ishijima, A.; Aida, T. *Angew. Chem., Int. Ed.* **2010**, *49*, 3030. (d) Suzuki, Y.; Okuro, K.; Takeuchi, T.; Aida, T. *J. Am. Chem. Soc.* **2012**, *134*, 15273. (e) Uchida, N.; Okuro, K.; Niitani, Y.; Ling, X.; Ariga, T.; Tomishige, M.; Aida, T. *J. Am. Chem. Soc.* **2013**, *135*, 4684. (f) Tamesue, S.; Ohtani, M.; Yamada, K.; Ishida, Y.; Spruell, J. M.; Lynd, N. A.; Hawker, C. J.; Aida, T. *J. Am. Chem. Soc.* **2013**, *135*, 15650. (g) Mogaki, R.; Okuro, K.; Aida, T. *Chem. Sci.* **2015**, *6*, 2802.

(11) Rana, T. M. *Nat. Rev. Mol. Cell Biol.* **2007**, *8*, 23.

(12) (a) DeRouchey, J.; Schmidt, C.; Walker, G. F.; Koch, C.; Plank, C.; Wagner, E.; Rädler, J. O. *Biomacromolecules* **2008**, *9*, 724. (b) Dohmen, C.; Edinger, D.; Fröhlich, T.; Schreiner, L.; Lächelt, U.; Troiber, C.; Rädler, J.; Hadwiger, P.; Vornlocher, H.-P.; Wagner, E. *ACS Nano* **2012**, *6*, 5198. (c) DeRouchey, J.; Walker, G. F.; Wagner, E.; Rädler, J. O. *J. Phys. Chem. B* **2006**, *110*, 4548.

(13) Forconi, M.; Herschlag, D. *Methods Enzymol.* **2009**, *468*, 91.

(14) Herce, H. D.; Garcia, A. E.; Cardoso, M. C. *J. Am. Chem. Soc.* **2014**, *136*, 17459.

(15) (a) Shimizu, H.; Hori, Y.; Kaname, S.; Yamada, K.; Nishiyama, N.; Matsumoto, S.; Miyata, K.; Oba, M.; Yamada, A.; Kataoka, K.; Fujita, T. *J. Am. Soc. Nephrol.* **2010**, *21*, 622. (b) Zuckerman, J. E.; Choi, C. H.; Han, H.; Davis, M. E. *Proc. Natl. Acad. Sci. U. S. A.* **2012**, *109*, 3137.

(16) Sonavane, G.; Tomoda, K.; Makino, K. *Colloids Surf., B* **2008**, *66*, 274.

DOI: 10.1021/jacs.5b08948
J. Am. Chem. Soc. 2015, 137, 15608−15611